Mostafa Mohammadabadi, Vikram Yadama*, LiHong Yao and Debes Bhattacharyya

Low-velocity impact response of wood-strand sandwich panels and their components

https://doi.org/10.1515/hf-2017-0169
Received October 20, 2017; accepted March 20, 2018; previously published online xx

Abstract: Profiled hollow core sandwich panels (SPs) and their components (outer layers and core) were manufactured with ponderosa and lodgepole pine wood strands to determine the effects of low-velocity impact forces and to observe their energy absorption (EA) capacities and failure modes. An instrumented drop weight impact system was applied and the tests were performed by releasing the impact head from 500 mm for all the specimens while the impactors (IMPs) were equipped with hemispherical and flat head cylindrical heads. SPs with cavities filled with a rigid foam insulation material (SP_{foam}) were also tested to understand the change in EA behavior and failure mode. Failure modes induced by both IMPs to SPs were found to be splitting, perforating, penetrating, core crushing and debonding between the core and the outer layers. SP_{foam}s absorbed 26% more energy than unfilled SPs. SP_{foam}s with urethane foam suffer less severe failure modes than SPs. SPs in a ridge-loading configuration absorbed more impact energy than those in a valley-loading configuration, especially when impacted by a hemispherical IMP. Based on the results, it is evident that sandwich structure is more efficient than a solid panel concerning impact energy absorption, primarily due to a larger elastic section modulus of the core's corrugated geometry.

Keywords: corrugated core, energy absorption, impact behavior, insulated sandwich panel, sandwich panel, sheathing material, wood-strand composite

***Corresponding author: Vikram Yadama,** Department of Civil and Environmental Engineering and Composite Materials and Engineering Center, Washington State University, Pullman, WA 99164, USA, Phone: +1 509 335 6261, e-mail: vyadama@wsu.edu
Mostafa Mohammadabadi: Material Science and Engineering Program and Composite Materials and Engineering Center, Washington State University, Pullman, WA 99164, USA
LiHong Yao: College of Material Science and Art Design, Inner Mongolia Agriculture University, Hohhot 010018, China
Debes Bhattacharyya: Department of Mechanical Engineering, The University of Auckland, Private Bag 92019, Auckland 1142, New Zealand

Introduction

Sandwich panels (SPs) consist of outer and core layers, made of different materials and which may have different geometries. The components are bonded to each other to form a composite, which has better properties than those of the sum of its parts. There are many types of SPs, such as ultra-lightweight foam core particle board SPs, wood-fiber-based tri-axial engineered sandwich composite panels, high-density fiberboard (HDF)-based SPs with a dual corrugated lightweight core, plywood-based SPs with maize granular in the core layer, just to mention a few (Smardzewski 2013; Shalbafan et al. 2013; Li et al. 2016; Smardzewski and Jasińska 2017; Burnett and Kharazipour 2018). The outer layers (facesheets) could be of materials that are strong and stiff to resist normal loads and bending moments, whereas the core layer should be light and flexible to resist shear forces. SPs are increasingly applied in aerospace, marine, automotive and building industries due to their lightweight, high flexural stiffness, good thermal insulation and noise reduction properties. SPs are seldom used for building construction but structural insulated panels with polystyrene or polyurethane foam are well suited to this application field. SPs with a three-dimensional (3D) fiberboard core and high- or medium-density fiberboards were also created by a wet process (Hunt and Winandy 2003). The disadvantages are lower structural performance and significant water demand for their production. The dry forming process has clear advantages (Weight and Yadama 2008a,b; Voth 2009; Rao et al. 2011, 2012; White 2011; Banerjee and Bhattacharyya 2011; Voth et al. 2015; Way et al. 2016). One of the most important applications of wood-strand SPs (WSSPs) having a 3D core and dry forming process could be as sheathing materials for building envelopes. Preliminary testing results of WSSPs (Voth 2009; White 2011; Voth et al. 2015) demonstrated that they have equal or better strength and stiffness properties than common sheathing materials such as oriented strand board (OSB) or plywood. In addition, creep test conducted on WSSPs confirmed their performance under long-term loads (Mohammadabadi et al. 2018). However, their behavior under impact loading during their service life is not yet determined. These kinds of tests are not trivial because SPs as building envelopes could behave as ductile materials under static loading, while under

impact loading they could behave more like brittle materials and be more susceptible to damages, such as puncturing, crushing, splitting and face/core debonding (Torre and Kenny 2000). Moreover, characterization of impact behavior and the subsequent failure mode of materials is complicated because many parameters, such as the shape and mass of the impactor (IMP), may influence the results (Mitrevski et al. 2006; Evci and Uyandiran 2017).

Low-velocity impact behavior was tested on SPs of various types, including foam-based ones with a variety of synthetic fiber outer plies (Hazizan and Cantwell 2002; Lim et al. 2004; Schubel et al. 2005; Imielińska et al. 2008; Navarro et al. 2012), honeycomb core (Qiao and Yang 2007), balsa wood (Atas and Sevim 2010) and corrugated core of glass and phenolics (Torre and Kenny 2000). Experimental work was done (Lim et al. 2004; Schubel et al. 2005; Qiao and Yang 2007; Imielińska et al. 2008; Atas and Sevim 2010; Navarro et al. 2012) as well as evaluations based on theoretical considerations (Hazizan and Cantwell 2002) and finite element analysis (Lim et al. 2004; Navarro et al. 2012). The results revealed that the failure modes are generally face fracture, core shear yield, core compressive yield and debonding between core and facesheet. SPs with glass/epoxy facesheets and balsa wood core are stiffer than those with polyvinyl chloride (PVC) core and wood cores provided a better shear performance. In fact, delamination is more likely in a foam core SP, due to the mismatch between the stiffness of top facesheets and PVC core, while local damage around the IMP is a common failure in SPs with balsa wood core. SP with a corrugated core can absorb higher impact energy without transferring high deformations to the inner structures.

Sheathing materials as part of walls can be subjected to impact loads due to collision with an airborne object during hurricanes or other high-wind events. On the other hand, in floors and roofs they can experience impacts due to a falling body (such as a hammer) during construction and service life. To our knowledge, there are no studies conducted on the impact behavior of WSSPs with thin wood-strand outer plies bonded to a thin-walled 3D wood-strand core (Figure 1) as described in the literature (Voth 2009; White 2011; Voth et al. 2015; Way et al. 2016; Mohammadabadi et al. 2018).

The objective of this study was to conduct a preliminary investigation of the low-velocity impact behavior of WSSPs and their components to understand the factors influencing this behavior. The individual components (outer and core layers) of the panels were impacted separately and the behavior of WSSPs with free cavities and WSSPs with rigid urethane foam in their cavities were reported separately.

Materials and methods

Preforms were produced from wood strands processed from ponderosa pine and lodgepole pine with 15.6–30.5 cm diameter at breast height. Because of their similarity, these species yield wood-strand composites of similar properties (Meyers 2001), and thus species differences were not considered. Wood strands, resinated with phenol formaldehyde (manufactured by Hexion Specialty Chemicals, Springfield, OR, USA), were hot-pressed to manufacture flat outer plies and a 3D core was hot-pressed in a matched-die compression mold. The core is a real 3D construction as its geometry is a biaxial corrugated shape with continuous ribs in the longitudinal direction and segmented ribs in the transverse direction. Flat outer plies were bonded to cores using a modified diisocyanate adhesive (Daubond U6000 series, manufactured by Daubert Chemical Company, Chicago, IL, USA) (Figure 1). A detailed description of the manufacturing process, including the forming of strand mats (preforms), moisture content, resin content and application, and the hot-pressing process is provided in the literature (Voth 2009; White 2011; Voth et al. 2015).

Figure 1: Wood strands, SP and its components and a rigid foam filled panel specimen.

Table 1: Average properties of wood-strand outer layers and the core normalized for a density of 640 kg/m³.

Property	n[a]	Average	COV (%)
E_L (GPa)	27	8.4	13.8
TS_L (MPa)	27	31	29.9
E_T (GPa)	26	2.8	29.5
TS_T (MPa)	26	9.3	47.8

[a]No. of specimens. E, Young's modulus; TS, tensile strength; the subscript letters L and T represent longitudinal and transverse directions, respectively.

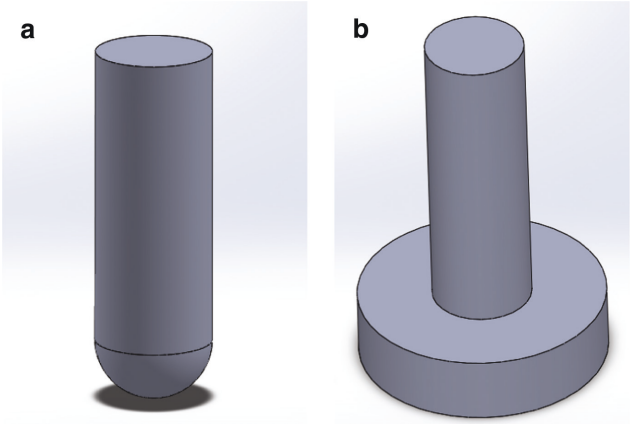

Figure 2: Impactors used for testing: (a) hemispherical and (b) flat head.

The average physical and mechanical properties are summarized in Table 1 (White 2011). The 3D core geometry resulted in hollow cavities within the SPs. In some of the SPs, the cavities were filled with a two-part rigid foam (Foam it Green) as described by White (2011).

Impact tests were conducted by means of the drop weight impact system (Imatek Drop Weight Impact Tester, Tower IM10-20), whose test bed size was 132×132 mm². All impact tests were performed by dropping weight from only one height. Hemispherical and flat head (Figure 2) IMPs were applied (IMP_{hemi} and $IMP_{fl.head}$, respectively) to study the effect of impact area (McNatt and Soltis 1990). The total mass and diameter of these IMPs were 13.826 kg and 25.4 mm, and 14.223 kg and 76 mm, respectively. The released height was 500 mm; therefore, the specimens were impacted at a potential energy level (E_p) of 67.75 J (hemispherical) and 69.7 J (flat head). The impact force was measured using a piezoelectric transducer. Velocity and displacement were computed by single and double integration of the acceleration as a function of time, respectively. Based on the computed velocity, the kinetic energy (E_K) of the IMP was measured (Eq. 1). Note that the kinetic energy at the collision moment is less than the potential energy because some energy is lost due to the friction between the IMP and the drop tower. Therefore, E_K is the maximum of available energy before impact.

$$E_K = \frac{1}{2} m V_i^2 < E_P = W h_0, \quad (1)$$

where W, m, h_0 and V_i are IMP weight, mass, initial drop height and velocity at the collision moment (initial velocity), respectively.

A unit cell can be defined as the simplest repeating element in the 3D core (Figure 3). Because of the 3D geometry, the thickness of the impacted face of an SP depends on how a specimen is oriented and loaded in the apparatus. The ridge and valley cases, in terms of the impact possibilities, are presented in Figure 3. The top layer is depicted transparent to show the difference between the two cases. As is visible, the impacted face for a ridge configuration will be thicker than that for a valley configuration.

The impact tests were conducted on four types of specimens including flat panel, 3D core, SP without a rigid foam in the cavities and SP with cavities filled with a rigid foam. Also, ridge and valley configurations were considered for both types of SP specimens (with and without foam). The same dimensions of one unit cell were considered for all specimens. The average dimensions of the specimens are presented in Table 2.

Force, displacement and absorbed energy are the resulting data of the impact tests, which were evaluated separately in terms of the SP components considering the cores with or without foam in combination with all testing parameters. Force and energy are presented with respect to displacement.

Results and discussion

Impact behavior of SP and its components

In the "force/energy vs. displacement" curves of SPs and their components impacted by two different IMPs (Figure 4), the maximum impact force is clearly visible. This is the maximum force that a specimen can resist,

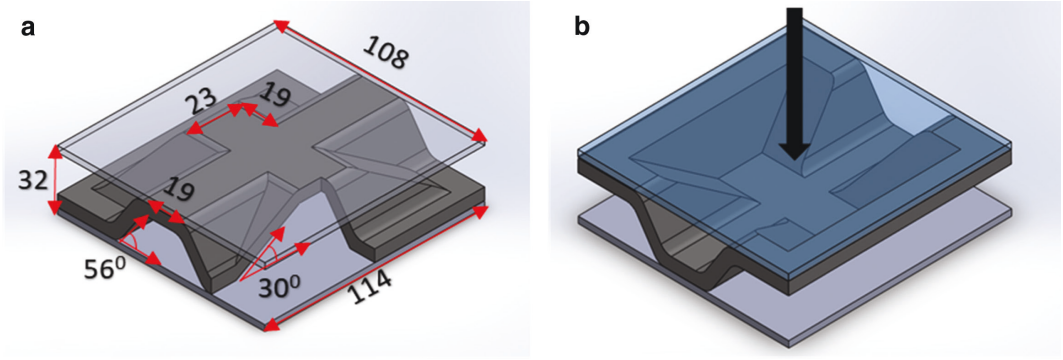

Figure 3: Loading configurations for a unit cell of the SP: (a) ridge and (b) valley (dimensions are in mm).

Table 2: Specimen configurations and average specimen dimensions.

Specimen type	n[a]	Length (mm)	Width (mm)	Thickness (mm)	Height (mm)
Flat ply	18	114	108	3.2	3.2
Corrugated panel	10	114	108	5.9	24.7
SP with and w/o foam	23	114	108	31.1	31.1

[a]No. of specimens.

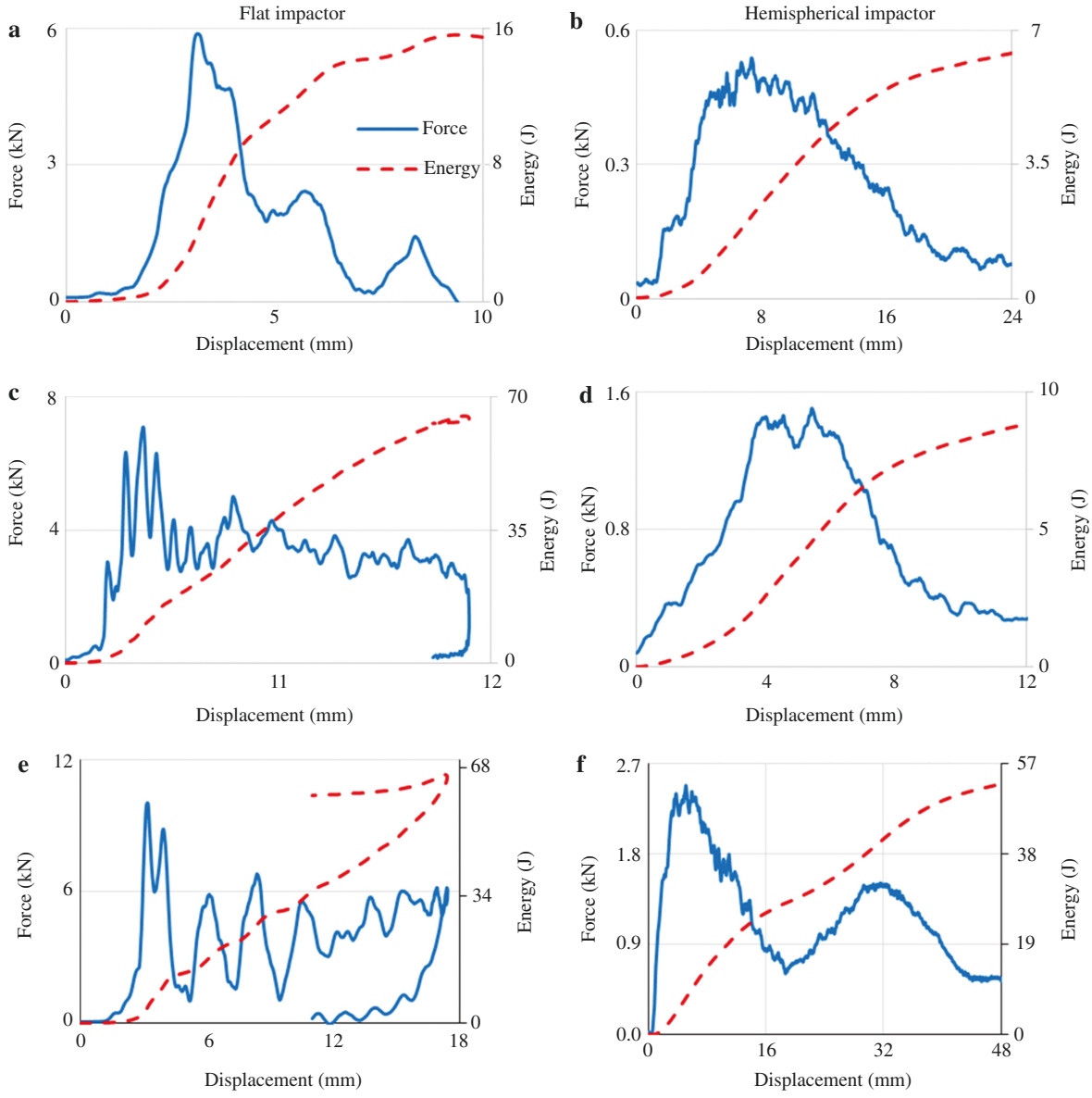

Figure 4: Force- and energy-displacement curves of different specimens (a and b) flat panel, (c and d) 3D core panel and (e and f) SP without foam in a ridge configuration.

and the absorbed energy associated with this force is the maximum energy. Total energy (E_T described in Eq. 2), which is different from maximum energy, represents the energy absorbed by the specimen:

$$E_T = 0.5\ \mathrm{m}\ (V_i^2 - V_f^2), \tag{2}$$

where V_f is the IMP velocity, when it passes through the specimen or rebounds (final velocity).

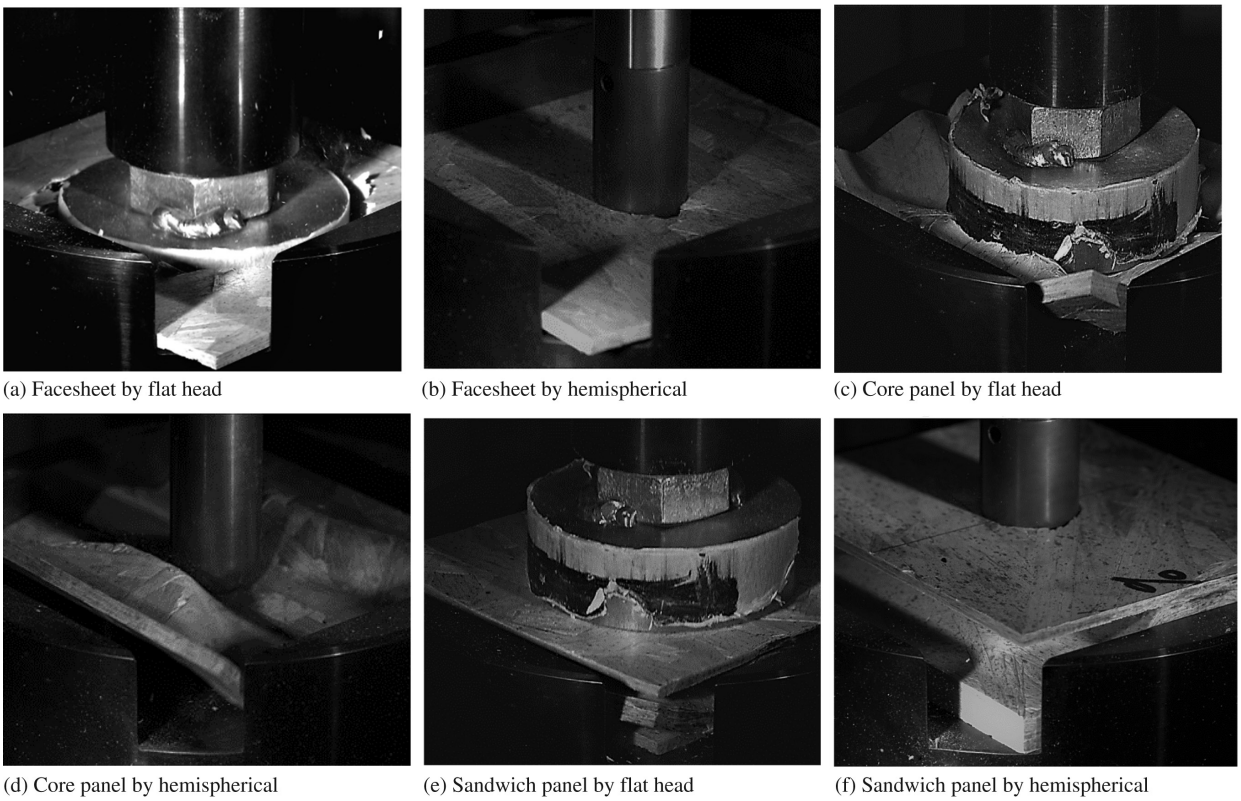

(a) Facesheet by flat head (b) Facesheet by hemispherical (c) Core panel by flat head

(d) Core panel by hemispherical (e) Sandwich panel by flat head (f) Sandwich panel by hemispherical

Figure 5: Failure modes of an SP and its components: (a) perforation, (b) perforation, (c) core crushing, (d) splitting, (e) debonding and core crushing and (f) perforation.

Regardless of the IMP type, the general trend of the force-displacement curve for flat outer and core layers (Figure 4a–d) has one major peak, whereas SPs (Figure 4e and f) display two predominant peaks. The first maximum force on the force-displacement curve of SP specimens impacted by $IMP_{fl.head}$ (Figures 4e and 5e) represents debonding between the core and the bottom facesheet, and the second one represents the core crushing. However, in the case of specimens loaded by the IMP_{hemi} (Figures 4f and 5f), the first load peak is a result of perforating the top facesheet and the core layer, and the second one is due to contacting the bottom facesheet by the IMP and perforating it.

Impact energy absorbed by a material causes an elastic deformation followed by an inelastic deformation and one or more mixed failure modes. If an IMP cannot punch through the specimen like in Figure 5c (one failure mode) and e (mixed failure mode), that amount of energy stored in the specimen as an elastic deformation will return to the IMP and result in IMP rebounding. Due to this effect, displacement on the corresponding force/energy curves (Figure 4c and e) is reduced. Also, the stored energy from the elastic deformation of the specimen returns to the IMP resulting in the total energy absorbed by the specimen dropping off as seen in Figure 4c and e.

The maximum forces and total energy values of all specimens (Table 3) impacted by $IMP_{fl.head}$ are higher because of the resistance provided by a larger contact area in contrast to an IMP_{hemi}, which results in a high stress intensity around the IMP. This causes localized damage in the SP and results in perforation (Figure 5b and f). However, SPs impacted by the $IMP_{fl.head}$ exhibit debonding and core crushing failure mode (Figure 5c and e) because of the distribution of impact load over a larger area.

The energy absorption (EA) level, determined by dividing the average total energy of each specimen configuration by the potential energy that specimen was subjected to (Eq. 3), is the percentage of potential energy absorbed by the specimen and dissipated during the impact test.

$$\mathrm{EA} = E_T / E_p, \tag{3}$$

EA levels of the specimens (Table 3) indicate that the IMP type has a significant effect on the EA of the core layer. The 3D geometry of the core layer dissipated on average 93% of the potential energy of the $IMP_{fl.head}$, whereas only 13% of it was lost in the case of IMP_{hemi}. A more concentrated impact load coupled with the cavity underneath the impact point (because of the 3D geometry of the core) led to a splitting failure (Figure 5d) and a lower energy loss. Regardless of

Table 3: Maximum force, maximum energy and total energy of SP and its components (values in parentheses are coefficients of variations).

Specimen	Impactor	n[a]	Max. force (kN)	Max. energy (J)	Total energy (J)	Energy abs. (%)
Outer layer	Hemisph	9	0.54 (20%)	2.13 (19%)	6.39 (21%)	9.4
	Flat head	9	5.88 (12%)	4.02 (32%)	15.6 (17%)	22.4
Core layer	Hemisph	5	1.51 (24%)	4.55 (33%)	8.86 (34%)	13.1
	Flat head	5	7.09 (40%)	8.25 (61%)	64.8 (2%)	93
SP w/o foam ridge config.	Hemisph	3	2.48 (20%)	7.78 (29%)	52.8 (24%)	78
	Flat head	3	10.1 (10%)	4.19 (28%)	66.2 (5%)	95.6
SP with foam ridge config.	Hemisph	3	3.67 (7%)	8.59 (4%)	66.6 (0.2%)	98.3
	Flat head	3	13.3 (10%)	17.1 (28%)	68.6 (1%)	98.4

[a]No. of specimens.

Table 4: Comparison between energy absorption of wood-strand composite and different materials impacted by a flat head impactor.

Specimen	Thickness t (mm)	Height h (mm)	t/h	Energy absorption level (%)[a]
Plywood[b]	19	19	1	67–94
OSB[b]	19	19	1	82–95
Flat ply	3.2	3.2	1	22
3D core	5.9	24.7	4.2	93
SP	31.1	31.1	1	95

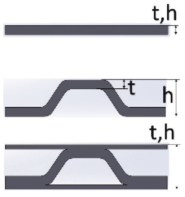

[a]Absorbed energy/impactor's potential energy. [b]McNatt and Soltis 1990.

the IMP type, SPs yield a higher energy loss and a better performance than the corrugated core specimens, while the flat panels perform poorly. A higher second moment of area due to out-of-plane strand deviations resulting from the 3D core geometry contributes to the higher toughness of the SPs and their higher EA levels.

The flat panels failed by perforating (Figure 5a and b), whereas the cores experienced either crushing (typically with $IMP_{fl.head}$, Figure 5c) or splitting (typically with IMP_{hemi}, Figure 5d). Typical failure modes of SPs were core crushing and debonding between the core and the outer layers (Figure 5e) and perforation (Figure 5f). When the maximum impact force (maximum energy) is reached, one of these failure modes is initiated and is continued until the IMP passes through the specimen or rebounds.

In a prior study (McNatt and Soltis 1990), the impact behavior of OSB and plywood specimens was tested by an $IMP_{fl.head}$ with a mass of 14 kg, impact area of a 76-mm diameter disk and the fall height was 500 mm (similar to the parameters in this study). As shown in Table 4, a comparison between the percentage of potential energy of IMP, that is absorbed by the specimens, indicates that a 3D core layer with significantly thinner walls has the capacity to absorb similar impact energy as commercially produced thicker wood composite sheathing materials because of the larger thickness to height ratio (meaning greater elastic section modulus). A 3D core geometry reduces material requirements and increases the EA capacity compared to a commercially produced OSB sheathing material of a relatively larger thickness. Moreover, when panel cavities are filled with foam, there is a trend toward a more consistent EA level as indicated by lower coefficients of variation of SP_{foam}s.

Effect of foam on the impact behavior of sandwich panel

Force- and energy-displacement curves of SP_{foam}s and their failure modes are presented in Figure 6. Foam in the cavities increases the SP's toughness and rebounds the IMP. The IMP_{hemi}, which perforated the SPs (Figure 5f), does not completely penetrate the SP_{foam}s but retracts. In the case of $IMP_{fl.head}$, the core crushing failure mode for SPs (Figure 5e) altered to a debonding failure mode (Figure 6b) in the case of SP_{foam}s. The behavior of SP_{foam} in terms of rebounding the IMP is similar to that of tough composite materials, such as graphite/epoxy, Kevlar/epoxy and glass fiber/polyester (Winkel and Adams 1985; Schubel et al. 2005).

Regardless of the IMP type, SP_{foam}s absorbed 98% of the energy exerted by the IMP (Table 2). The maximum force and total absorbed energy of SP_{foam}s compared to those of SPs increased by 48% and 26%, respectively, when impacted by IMP_{hemi}, and around 32% and 4% in the case of $IMP_{fl.head}$. Filling the SP cavities with foam improves the efficiency of an SP by increasing its maximum force capacity and EA and by changing its failure mode from a severe (perforation and crushing) to a less severe one (penetration and debonding).

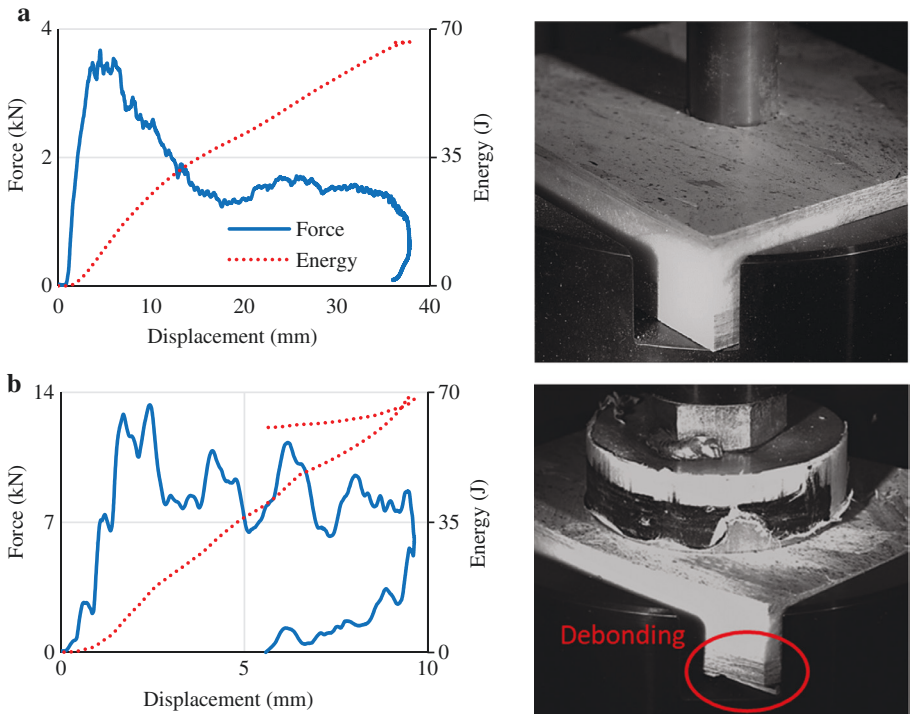

Figure 6: Force- and energy-displacement curves of SPs with foam in a ridge-loading configuration and associated failure modes: (a) hemispherical impactor, penetration mode, and (b) flat impactor, debonding mode.

Effect of loading configuration on the impact behavior

Two different loading configurations (ridge and valley) are possible for the SP specimens (Figure 3). The total EA of an SP specimen in a valley-loading mode is lower than that in a ridge-loading mode (Figure 7), due to a thicker wall on the impact side of a ridge-loading configuration, where core and facesheets are bonded together. The reductions for SPs with and without foam are ca. 25% and 15%, respectively, if they were impacted by IMP_{hemi}. However, for an SP without foam, impacted by $IMP_{fl.head}$, the reduction of EA was 3%, which is not significant considering the margin of experimental errors and material variation. The impact behavior of an SP used as a sheathing material would depend on the location of the impact force, especially when impacted by objects that tend to have a concentrated impact comparable to that of IMP_{hemi}. However, the effect of loading configuration on the reduction of impact behavior could be offset significantly with the inclusion of foam in the cavities.

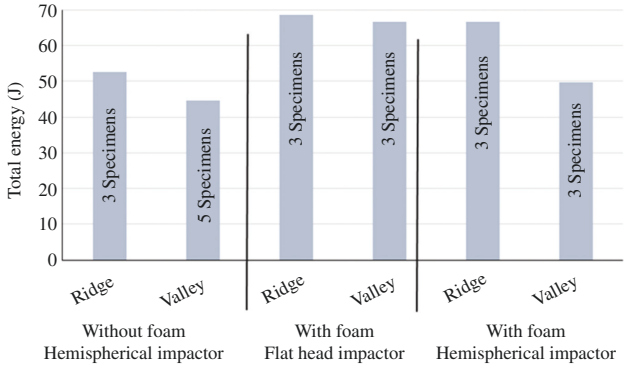

Figure 7: Effect of loading configuration on total energy absorbed by SPs.

Conclusions

The behavior of a WSSP with and without foam and its components (outer flat ply and inner 3D core layer) impacted by hemispherical and flat head IMPs was evaluated. The 3D geometry of the core layer yields a higher section modulus and enables it to absorb more energy than a flat outer layer, especially when impacted by a flat head IMP. Regardless of the IMP type, the inclusion of a rigid foam has a positive effect on the impact performance of the SPs, and alters the failure mode from a severe to a less severe one. Those panels impacted in a ridge-loading configuration absorb more energy than those impacted in a valley configuration because of the thicker wall on

the impact side and greater stability provided by the core walls. SPs with and without foam in a ridge-loading configuration impacted by hemispherical IMP absorb 25% and 15% more energy than those in a valley configuration. Typical failure modes are perforation, splitting, core crushing, penetration and debonding between the core and the outer layer. However, only penetration and debonding between the core and the outer layer were observed for SPs filled with foam. SPs with their 3D wood-strand core and cavities filled with foam are more effective than OSBs as sheathing materials.

Acknowledgments: Our gratitude to the Centre for Advanced Composite Materials (CACM) at the University Of Auckland, New Zealand, for letting us use the impact testing equipment. The authors would also like to thank Mr. Jos Geurts of CACM for his help and guidance during the impact testing. This material is based upon work partially supported by the National Science Foundation under Grant No. CMMI-1150316 (Funder Id: 10.13039/100000147).

Author contributions: All the authors have accepted responsibility for the entire content of this submitted manuscript and approved submission.
Research funding: None declared.
Employment or leadership: None declared.
Honorarium: None declared.

References

Atas, C., Sevim, C. (2010) On the impact response of sandwich composites with cores of balsa wood and PVC foam. Compos. Struct. 93:40–48.

Banerjee, S., Bhattacharyya, D. (2011) Optimal design of sandwich panels made of wood veneer hollow cores. Compos. Sci. Technol. 71:425–432.

Burnett, M., Kharazipour, A. (2018) Mechanical behaviour of a lightweight, three-layered sandwich panel based on the raw material maize. Holzforschung 72:65–70.

Evci, C., Uyandıran, İ. (2017) The effect of the impactor diameter and temperature on low velocity impact behavior of CFRP laminates. In: AIP Conference Proceedings. AIP Publishing, College Park, MD. Vol. 1809, No. 1, p. 020014.

Hazizan, M.A., Cantwell, W.J. (2002) The low velocity impact response of foam-based sandwich structures. Compos. Part B 33:193–204.

Hunt, J.F., Winandy, J.E. (2003) 3D engineered fiberboard: engineering analysis of a new building product. Proc. EcoComp., Queen Mary, Univ. of London, London. pp. 1–8.

Imielińska, K., Guillaumat, L., Wojtyra, R., Castaings, M. (2008) Effects of manufacturing and face/core bonding on impact damage in glass/polyester-PVC foam core sandwich panels. Compos. Part B 39:1034–1041.

Li, J., Hunt, J.F., Gong, S., Cai, Z. (2016) Fatigue behavior of wood-fiber-based tri-axial engineered sandwich composite panels (ESCP). Holzforschung 70:567–575.

Lim, T.S., Lee, C.S., Lee, D.G. (2004) Failure modes of foam core sandwich beams under static and impact loads. J. Compos. Mater. 38:1639–1662.

McNatt, J.D., Soltis, L.A. (1990) Instrumented impactor for testing wood-base floor panels. J. Test. Eval. 18:265–273.

Meyers, K.L. (2001) Impact of strand geometry and orientation on mechanical properties of strand composites. MS Thesis, Dept. of Civil and Env. Eng., Washington State University, WA, USA.

Mitrevski, T., Marshall, I.H., Thomson, R. (2006) The influence of impactor shape on the damage to composite laminates. Compos. Struct. 76:116–122.

Mohammadabadi, M., Yadama, V., Geng, J. (2018) Creep behavior of 3D core wood-strand sandwich panels. Holzforschung. https://doi.org/10.1515/hf-2017-0088. [Epub ahead of print].

Navarro, P., Marguet, S., Ferrero, J.F., Barrau, J.J., Lemaire, S. (2012) Modeling of impacts on sandwich structures. Mech. Adv. Mater. Struct. 19:523–529.

Qiao, P., Yang, M. (2007) Impact analysis of fiber reinforced polymer honeycomb composite sandwich beams. Compos. Part B 38:739–750.

Rao, S., Jayaraman, K., Bhattacharyya, D. (2011) Short fibre reinforced cores and their sandwich panels: processing and evaluation. Compos. Part A 42:1236–1246.

Rao, S., Jayaraman, K., Bhattacharyya, D. (2012) Micro and macro analysis of sisal fibre composites hollow core sandwich panels. Compos. Part B 43:2738–2745.

Schubel, P.M., Luo, J.J., Daniel, I.M. (2005) Low velocity impact behavior of composite sandwich panels. Compos. Part A 36:1389–1396.

Shalbafan, A., Lüdtke, J., Welling, J., Frühwald, A. (2013) Physio-mechanical properties of ultra-lightweight foam core particleboard: different core densities. Holzforschung 67:169–175.

Smardzewski, J. (2013) Elastic properties of cellular wood panels with hexagonal and auxetic cores. Holzforschung 67:87–92.

Smardzewski, J., Jasińska, D. (2017) Mathematical models and experimental data for HDF based sandwich panels with dual corrugated lightweight core. Holzforschung 71:265–273.

Torre, L., Kenny, J.M. (2000) Impact testing and simulation of composite sandwich structures for civil transportation. Compos. Struct. 50:257–267.

Voth, C.R. (2009) Lightweight sandwich panels using small-diameter timber wood-strands and recycled newsprint cores. MS Thesis, Dept. of Civil and Env. Eng., Washington State University, WA, USA.

Voth, C., White, N., Yadama, V., Cofer, W. (2015) Design and evaluation of thin-walled hollow-core wood-strand sandwich panels. J. Renew. Mater. 3:234–243.

Way, D., Sinha, A., Kamke, F.A., Fujii, J.S. (2016) Evaluation of a wood-strand molded core sandwich panel. J. Mater. Civ. Eng. 28:04016074.

Weight, S.W., Yadama, V. (2008a) Manufacture of laminated strand veneer (LSV) composite. Part 1: Optimization and characterization of thin strand veneers. Holzforschung 62:718–724.

Weight, S.W., Yadama, V. (2008b) Manufacture of laminated strand veneer (LSV) composite. Part 2: Elastic and strength properties of laminate of thin strand veneers. Holzforschung 62:725–730.

White, N.B. (2011) Strategies to improve thermal and mechanical properties of wood composites. MS Thesis, Dept. of Civil and Env. Eng., Washington State University, WA, USA.

Winkel, J.D., Adams, D.F. (1985) Instrumented drop weight impact testing of cross-ply and fabric composites. Composites 16:268–278.